# Spatial competition: roughening of the ecological interface

November 14, 2014

Andrew J. Allstadt,[1,⋆] Jonathan A. Newman,[2,§] Jonathan A. Walter,[3,♯] G. Korniss,[4,‡] and Thomas Caraco[5,†]

1. Department of Forest and Wildlife Ecology, University of Wisconsin-Madison, Madison WI 53706, USA

2. School of Environmental Sciences, University of Guelph, Guelph, Ontario N1G 2W1, Canada

3. Department of Environmental Sciences, University of Virginia, Charlottesville, VA 22904-4123, USA

4. Department of Physics, Applied Physics, and Astronomy,
Rensselaer Polytechnic Institute, 110 8th Street, Troy NY 12180-3590, USA

5. Department of Biological Sciences, University at Albany, Albany NY 12222, USA

⋆Corresponding author, e-mail: allstadt@wisc.edu; §e-mail: jonathan.newman@uoguelph.ca; ♯e-mail: jaw3es@virginia.edu; ‡e-mail:korniss@rpi.edu; †e-mail: tcaraco@albany.edu.

Biological Science: Ecology

*Keywords*: ecological invasion, front-runner, interface roughening, scaling laws, spatial competition

*Abstract.* Limited dispersal distance, whether due to vegetative growth or localized reproduction, generates spatial clustering. Many invasive plants, in particular, propagate clonally and aggregate spatially. Local dispersal concentrates intraspecific interactions within clusters, while most between-species interactions occur near cluster boundaries. Spread of a spatially clustered, invasive plant then becomes motion of an interface between the invader and resident species, and competition along the interface produces random variation in the extent of invasive advance. Development of these growth fluctuations, termed stochastic roughening, will often structure the ecological interface as a self-affine fractal. This property implies a series of scaling relationships for the statistics of spatial growth. For many individual-based processes exhibiting both forward and lateral propagation, the extent of invader advance becomes spatially correlated along the interface, and the width of the interface (where invader and resident compete directly) increases as a power function of time. Once roughening equilibrates, interface width and the location of the most advanced invader (the "front-runner") beyond the mean incursion should both increase as a power function of interface length. To test these predictions, we let white clover (*Trifolium repens*) invade ryegrass (*Lolium perenne*) experimentally. Spatial correlation developed as anticipated, and both interface width and the front-runner's lead scaled as a power law of length. However, the scaling exponents differed, plausibly an effect of clover's growth morphology. Our results suggest that the theory of kinetic roughening offers a framework for understanding causes and consequences of spatial pattern in between-species interaction. Although our analysis focuses on growth at the neighborhood scale, the methods may be applied to invasive fronts at extended spatial scales.

# 1 Introduction

Pattern analysis of plant communities commonly reveals spatial mosaics generated by clustered growth of individual species [Cain et al. 1995, Dale 1999, Condit et al. 2000]. Clustering may follow a template set by environmental heterogeneity, if different locations favor different species [Snyder and Chesson 2003], but more often, dispersal limitation aggregates conspecific individuals [Harada and Iwasa 1994]. For example, most invasive plants are clonal and propagate vegetatively [Sakai et al. 2001, Liu et al. 2006], so that invaders initially cluster among residents [Cantor et al. 2011].

Individual plants usually compete at the nearest-neighbor scale [Goldberg and Barton 1992, Levine et al. 2004]. Given local competition, clustering influences interaction frequencies and the consequent population dynamics [Herben et al. 2000, Chesson and Neuhauser 2002]. When different species each aggregate spatially and interact locally, intraspecific competition should predominate within clusters, while interspecific competition will localize at the interface between clusters [Chesson 2000, Murrell and Law 2003, Yurkonis and Meiners 2004]. This interaction geometry implies that the advance *versus* extinction of a rare competitor may depend on development and movement of a between-species interface [Gandhi et al. 1999, Korniss and Caraco 2005]. That is, we envision a non-equilibrium system where increase or decline in a species' abundance drives interface motion.

An invading species' density declines from positive equilibrium to rarity across the width of an ecological interface [O'Malley et al. 2006]. As a competitively superior invader excludes the resident within the width, the front is pushed forward. Given this simple picture, we ask how varying the length of the interface affects statistical properties of an

invader-resident interaction. We emphasize the relative position of the "front-runner," the furthest advanced invader, a metric used in both theoretical and applied invasion ecology [Hajek et al. 1996, Clark et al. 2001, Thomson and Ellner 2003].

We treat invasive growth as dispersal-limited stochastic process; our analysis takes the invader as competitively superior to the resident. We assume that the ecological interface, once roughening has equilibrated, has a particular fractal geometry [Family and Vicsek 1985, Barabási and Stanley 1995, Cannas et al. 2004]; see Section 2. This assumption has quantitative ecological implications; it predicts that both interface width and the front-runner's lead will increase as a power function of the length of the advancing front [O'Malley et al. 2009a].

The next section describes our application of kinetic roughening to ecology. Section 3 reports an experiment testing predicted scaling relationships; we let Dutch white clover (*Trifolium repens*) advance into plots of perennial ryegrass (*Lolium perenne*). Our results suggest a simplifying generalization concerning the spatial organization of local competitive interactions. Although we apply kinetic roughening at the scale of clonal-plant clusters, the same methods might help organize understanding of invasive fronts at greater scales.

## 2 Local Dispersal and Interface Roughening

A dispersal-limited invader's population growth typically begins as small, nearly circular clusters of individuals. Despite an invader's competitive advantage, some small clusters will disappear due to demographic stochasticity. But clusters exceeding a critical size will continue to grow and displace the resident [Allstadt et al. 2007]. After a single cluster attains sufficient size, or after large clusters coalesce, we can treat the perimeter as a

1-dimensional front that has roughened during advance [O'Malley et al. 2009a]. Some
70 invasions move perpendicularly to a road or shore; they can be treated as initially linear
[Cannas et al. 2004]. The dynamics of an ecological interface distinguishes it from an
72 ecotone, when the latter implies a change in species composition due to abiotic factors that
vary slowly relative to the timescale of population growth
74 [Gastner et al. 2009, Eppinga et al. 2013].

Given an initially linear front, development of spatially correlated growth along an
76 interface is termed stochastic roughening [Kardar et al. 1986, Barabási and Stanley 1995].
Roughening and dynamic scaling offer a useful framework for identifying dynamics shared
78 by correlated growth processes differing in details of local interactions. Applications span
processes in physical materials [Barabási and Stanley 1995], biological tissues
80 [Galeano et al. 2003, Ranft et al. 2014], parallel-computing and information systems
[Korniss et al. 2000, Korniss et al. 2003], and ecological invasion
82 [Cannas et al. 2004, O'Malley et al. 2006]. When we analyze the front-runner's location,
correlated fluctuations along the interface are quite important, since traditional
84 extreme-value statistics [Fisher and Tippett 1928, Galambos et al. 1994], developed for
*independent* random variables, do not apply [Majumdar and Comtet 2004]. Figure 1 shows
86 an interface from our field experiment. Invasive growth along the interface clearly roughens
with time. The plots also suggest correlated advance at nearby locations.

## 88 2.1 Interface roughening: development and saturation

To apply concepts of statistical physics [Kardar et al. 1986, Barabási and Stanley 1995] to
90 spatial competition, we first define interface attributes and describe development of a
roughened interface. Then we address scaling relationships at equilibrium (after

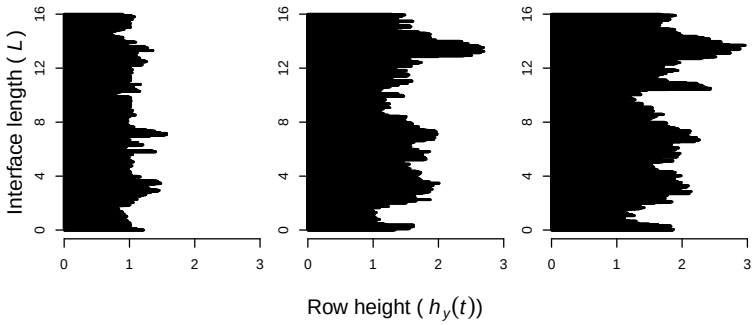


Figure 1: Roughening of clover interface. White clover (*T. repens*, black area) advancing into perennial ryegrass (*L. perenne*), from photographs taken during experiment. Interface length $L \equiv L_y = 16$ $m$. Row heights $h_y(t)$ in $m$. June (left), August (center) and October (right) 2010 shown. The interface advances, left to right, and roughens; neighboring heights suggest spatial correlation.

| Symbols | Definitions |
|---|---|
| $L_x,\ L_y(=L)$ | Lattice size ($L$ = interface length = front length) |
| $t$ | time |
| $h_y(t)$ | Rightmost invader in row $y$ at time $t$ |
| $\overline{h}(t)$ | Mean of $h_y(t)$ (the average is taken across all rows $y$) |
| $h_{max}(t)$ | Rightmost invader at time $t$ |
| $\Delta_{max}(t) = h_{max}(t) - \overline{h}(t)$ | Distance from front-runner to mean of front |
| $\langle w^2 \rangle$ | Mean squared interface width |
| $\xi(t)$ | Correlation length along interface |
| $t_\times$ | Crossover time, where $w^2$ equilibrates |
| $\alpha$ | Roughness exponent |
| $\beta$ | Growth exponent |
| $z$ | Dynamic exponent |

Table 1: Definitions of variables.

roughening "saturates"). Table 1 lists symbols we use.

Discrete ("individual-based") models capture effects of nonlinearity and stochasticity inherent to a dispersal-limited invader's dynamics at an ecological interface [Antonovics et al. 2006, Pachepsky and Levine 2011]. Therefore, we characterize front roughening as a lattice based process. Our description applies across a variety of individual-based models for growth at an interface [Plischke et al. 1987, O'Malley et al. 2009a].

An $L_x \times L_y$ rectangular lattice represents a habitat occupied by resident and invader species. Each lattice site is either occupied by the invader, occupied by the resident, or empty. Mortality of either species opens occupied sites. An empty site becomes occupied through propagation from a nearest-neighboring occupied site. Restricting propagation to nearest neighbors, of course, imposes dispersal-limitation. The invader's competitive superiority drives interface motion. If invader-resident competition is preemptive only, the invader has the lower mortality/propagation ratio [Allstadt et al. 2009]. If competition combines site preemption and direct interference, the species' demographic rates satisfy conditions in Allstadt et al. [2012].

Suppose that the invader initially occupies only a few vertical columns at the left edge of the lattice; all other sites are occupied by the resident or open. Invasive advance occurs in the $x$-direction. Importantly, neighborhood geometry (the dispersal constraint) permits both forward and lateral growth. The former pushes the front, and the latter generates spatial correlation along the front [Kardar et al. 1986, Barabási and Stanley 1995]. That is, lateral growth of advanced heights tends to increase height in adjacent rows.

We let $L \equiv L_y$, interface length (hence, front length). At time $t$, $h_y(t)$ is the location of the most advanced (right-most) invader in row $y$; $y = 1, 2, ..., L$. The front's average location is the mean height among rows, $\overline{h}(t) = \sum_y h_y(t)/L$. We take longitudinal system size $L_x$ as sufficiently large that it does not affect population processes.

Figure 2 shows the width of the interface about the invader's average incursion $\overline{h}(t)$. To quantify roughening, we define the width of the interface *via*:

$$w^2(L,t) = \frac{1}{L}\sum_{y=1}^{L}[h_y(t) - \overline{h}(t)]^2 \qquad (1)$$

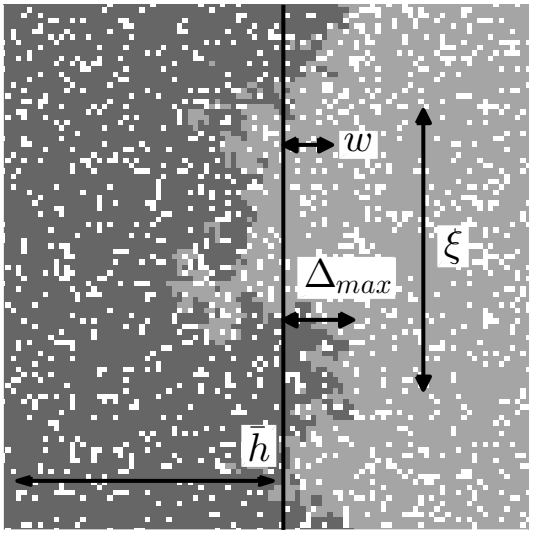


Figure 2: Interface attributes. Width ($w$) and the extreme advance ($\Delta_{max}$) relative to the mean front position ($\overline{h}$) in a rough front. For illustration, correlation length $\xi$ is also indicated. Dark: invader, medium: resident and white: open.

Roughness $w^2(L,t)$ itself varies stochastically, and we represent its expectation (averaged over realizations of intrinsic noise) at time $t$ by $\langle w^2(L,t)\rangle$. We take $w = \sqrt{\langle w^2(L,t)\rangle}$ as the width of the front, the typical extent of the interface parallel to the direction of advance.

Power-law scaling relationships should characterize an interface with spatially correlated heights. Importantly, these properties do not, in general, depend on details of the local growth dynamics [Family and Vicsek 1985, Kardar et al. 1986]. That is, variation in demographic processes among different invader-resident systems should exhibit the same qualitative scaling effects [Cannas et al. 2004, O'Malley et al. 2009a]. Spatially correlated heights imply that the interface should equilibrate as a self-affine fractal; this structure produces ecologically interesting scaling laws. A roughened, self-affine interface (or anisotropic fractal) has a width $w(L)$, where $L$ is front length. Suppose that we increase length according to $L \to kL$. Then interface width must be re-scaled according to $w \to k^{\alpha}w$ to preserve statistical invariance ("look the same" at different scales). Length and width must be increased by different factors, and the transformation has a power-law

134 form. Numerical calibration of the scaling laws can, of course, differ across species and environments, but it is the general relationships we emphasize.

## 136 2.2 Interface development

As the invader begins to advance, the interface starts to roughen, and invader heights $h_y(t)$ 138 become dependent random variables. That is, a single correlation length $\xi(t)$ develops along the interface (Fig. 2). Correlation length initially increases with time according to 140 the power-law scaling $\xi(t) \sim t^{1/z}$ [Majumdar and Comtet 2005], where $z$ is called the dynamic exponent. Once $\xi(t)$ spans the length $L$ of the interface, "crossover" occurs. The 142 interface continues to advance, but roughening has reached statistical equilibrium (roughening "saturates" at crossover) [Barabási and Stanley 1995]. The duration of 144 interface development, termed crossover time $t_\times$, increases with interface length; the power-law scaling is $t_\times \sim L^z$. The development of interface width offers a more easily 146 tested prediction. Prior to saturation, interface width $w$ exhibits temporal scaling behavior according to $w \sim t^\beta$. $\beta$ ($\beta > 0$) is called the growth exponent.

148 Spatially correlated growth, shaped by limited dispersal and neighborhood-scale competition, underlies fractal structure of an interface. The height-height correlation 150 function (Pearson correlation) is:

$$G_t(l) = \frac{\left\langle \left(h_{y+l}(t) - \overline{h}(t)\right)\left(h_y(t) - \overline{h}(t)\right)\right\rangle_y^{1/2}}{\left\langle \left(h_y(t) - \overline{h}(t)\right)^2\right\rangle_y^{1/2}} \ . \tag{2}$$

We use $G_t(l)$ to estimate correlation length $\xi(t)$ along the interface; height-height 152 correlation should decline as distance $l$ between rows increases.

We monitor the roughening associated with increasing correlation distance along the developing interface in two ways; each combines results from windows of length $l < L$. The local width, $w_t(l)$, is the average interface width estimated across an ensemble of portions of the interface, each with length $l$. The local width at time $t$ is given by:

$$w_t(l) = \left\langle \left( h_y(t) - \bar{h}(y,t) \right)^2 \right\rangle_y^{1/2} \quad . \tag{3}$$

The height-difference correlation function [Karabacak et al. 2001] integrates roughness during both development and saturation. The height-difference correlation function, at time $t > 0$, is given by:

$$C_t(l) = \left\langle \left( h_{y+l}(t) - h_y(t) \right)^2 \right\rangle_y^{1/2} \quad . \tag{4}$$

Each average $w_t(l)$ and $C_t(l)$ is taken across all rows $y$. For $l < \xi(t)$, both $w_t(l)$ and $C_t(l)$ exhibit power-law scaling over distances along the interface: $w_t(l),\ C_t(l) \sim l^{\alpha}$. $\alpha$ ($\alpha > 0$) is the roughness exponent, and characterizes the fractal nature of the interface [Barabási and Stanley 1995]. As the interface roughens with time, the correlation distance $\xi$ increases. Consequently, the linear dependence of $\ln w_t(l)$ and $\ln C_t(l)$ on $\ln l$, with slope $\alpha$, should extend to greater lengths $l$ along the interface, until saturation.

## 2.3 The saturated interface

After crossover ($t > t_{\times}$), steady-state properties of the interface depend on its length $L$ [Schehr and Majumdar 2006]. Interface width $w$ scales with interface length according to $\langle w^2(L,\infty)\rangle \sim L^{2\alpha}$; interface width increases as a power function of its length, according to the roughness exponent $\alpha$.

Note that we do not predict roughness *per se*, but ask how roughening changes from a

shorter to a longer interface. Power-law scaling for $\langle w^2(L,\infty)\rangle$ permits us to ask novel questions about invasive spatial growth. Cannas et al. [2004] hypothesize that life-history variation among invading tree species might influence the roughness exponent. Our analysis emphasizes how scaling of width with interface length organizes within and between-species interactions, and how the expected location of the invader's extreme advance depends on interface length.

In general, the scaling exponents are interdependent: $\alpha = \beta z$ [Kardar et al. 1986]. Dependence arises from the self-affine structure of the interface. Random demographic events render the interface disorderly, and we assume that the interface equilibrates as an anisotropic fractal [Barabási and Stanley 1995]. "Random demographic events" means local processes including both forward and lateral invader growth. As we noted, forward growth pushes invasive advance, and lateral growth builds spatial correlations between heights. Without lateral growth, each $h_y(t)$ becomes an independent birth-death process, implying no spatial correlation.

## 2.4 Roughening, scaling and the front-runner

The pace of invasive advance remains an issue in basic and applied ecology [Shigesada et al. 1986, van den Bosch et al. 1992]. Deterministic reaction-diffusion models offer approximate velocities, but assume continuous densities, and so cannot appreciate consequences of spatially correlated variability in a dispersal-limited invader's advance [Clark et al. 2003, Antonovics et al. 2006]. Dispersal limitation reduces velocity, compared to the reaction-diffusion alternative [Moro 2001, Escudero et al. 2004], but analytic approximation of a discrete, stochastic model's interface velocity remains a challenge [Pechenik and Levine 1999], especially for two-dimensional environments.

Krug and Meakin [1990] found that a discrete model's *reduction* in velocity, relative to the reaction-diffusion wave-speed, varies inversely with interface length. But no scaling relationship for either a discrete model's interface velocity or velocity reduction due to dispersal limitation is available. Interface velocity depends on specific details governing local (*i.e.*, individual-level) propagation and mortality [Moro 2001]. For our purposes, an important point is that scaling laws involving the roughness exponent $\alpha$ do not depend on invasion speed [Barabási and Stanley 1995].

## 2.5 The front-runner: scaling of extremes

The maximal invasive advance defines the front-runner's position. At time $t$ we locate the front-runner at $h_{max}(t) = \max_y\{h_y(t)\}$. Given mean interface height $\overline{h}(L,t)$, the invader's maximal relative advance at time $t$ is $\Delta_{max}(L,t) = h_{max}(t) - \overline{h}(L,t)$. We assume that roughening equilibrates before considering the scaling of the expected lead $\langle\Delta_{max}\rangle_L$; note dependence on interface length $L$.

The probability density of the front-runner's excess $\Delta_{max}(L,t)$ has been obtained analytically [Majumdar and Comtet 2004, Majumdar and Comtet 2005]. For broad classes of dispersal-limited stochastic growth models, the scaled variable $\Delta_{max}/\langle\Delta_{max}\rangle$ has an Airy probability density, and the steady-state average excess of the front-runner over the mean height scales with interface length exactly as does the width. That is, $\langle\Delta_{max}\rangle_L \sim L^{\alpha}$. Furthermore, we can infer the size of the extremes for an interface of linear size $L$ with estimates obtained in limited observation windows with size $L_{\text{obs}}$. We have: $\langle\Delta_{max}(L)\rangle \approx \langle\Delta_{max}(L_{\text{obs}})\rangle k^{\alpha}$, where $k = (L/L_{\text{obs}})$, by the properties of a self-affine interface [O'Malley et al. 2009b]. Table 2 collects scaling relationships we study.

| Regime | Prediction | Comment |
|---|---|---|
| *Development* | $\xi(t) \sim t^{1/z}$ | Correlation length, dynamic exponent |
| | $w_t \sim t^{\beta}$ | Interface width, growth exponent |
| | $t_{\times} \sim L^{z}$ | Crossover time, interface length |
| | $C_t(l) \sim l^{\alpha}$ | Height-difference correlation, $l < \xi(t)$ |
| *Stationarity* | $w \sim L^{\alpha}$ | Interface width, roughness exponent |
| | $\langle \Delta_{max} \rangle_L \sim L^{\alpha}$ | Front-runner's lead |
| | $\beta = \alpha / z$ | Self-affine fractal |

Table 2: Predicted scaling relationships. The interface roughens during development. After spatial correlation spans interface length, interface width remains statistically stationary.

# 3 Methods

We studied dispersal-limited competition between Dutch white clover (*T. repens*) and perennial ryegrass (*L. perenne*). Both species reproduce mainly through local, clonal growth [Turkington et al. 1979, Schwinning and Parsons 1996a]. *T. repens* propagates vegetatively through stoloniferous stems [Fraser 1989], while *L. perenne* produces tillers [Fustec et al. 2005]. Competitive interaction between these important forage crops is well understood [Cain et al. 1995, Schwinning and Parsons 1996b]. We located experimental plots at the University of Guelph Turfgrass Institute in an area homogeneous with respect to micro-topography ($43°33'N, 80°13'W$). To minimize spatial heterogeneity, vegetation and top layer of soil were removed, and the soil tilled before the experiment began.

## 3.1 Experimental design

We established plots with interface length $L = 1$, 2, 4, 8, and 16 $m$, with four replicates of each length. To avert edge effects, we added a 0.5 $m$ buffer, where no data were collected, at both ends of every plot. A plot had dimensions of $L \times 3$ $m$; all plots were initially split lengthwise by plastic dividers into sections of 1 $m$ and the remaining 2 $m$. We planted *T. repens* in the one-meter sections, and *L. perenne* in the two meter sections; we anticipated

that clover would advance, given the soil resources and occasional mowing. Appendix A
234 details experimental methods.

By spring 2009 mono-cultures were established, and we removed the plastic barriers
236 between species. In June 2010 we began recording the monthly advance of *T. repens* in each plot. We resolved measurements at a scale of 1 $cm^2$, the size of an individual clover
238 ramet [Silvertown 1981]. We marked each 1 $m^2$ subsection of every plot permanently, to reference growth measurements. Each such subsection was photographed from above after
240 monthly mowing. We re-projected each photo to correct for perspective, and combined photos from the same plot. We recorded row heights $h_y(t)$ for *T. repens* in each plot, and
242 noted the front-runner's lead on the mean clover height.

We tested power-law relationships against alternative linear and exponential models
244 [Solow et al. 2003]. Additionally, we fit power-law models with two different assumptions regarding error distribution. The first assumed normally distributed, additive error; the
246 second assumed log-normally distributed, multiplicative error [Xiao et al. 2011]. Our scaling laws, Table 2, predict the latter. We compared relative support for each model
248 using differences in AIC scores ($\Delta AIC$); we considered models with $\Delta AIC < 2$ as supported substantially [Burnham and Anderson 2002].

## 250 4 Results

During the 2010 growing season, clover advanced rapidly; several longer fronts approached
252 the far end of the plot by October. Figure 3A shows each plot's mean height $\overline{h}(t)$ against time. Overall mean clover height increased for five consecutive months. However, several
254 clover fronts began to experience winter die-back in October. Therefore, our analysis

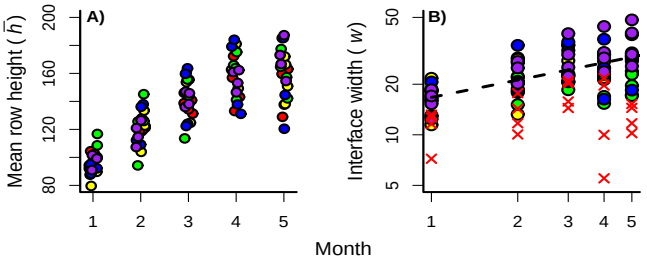


Figure 3: Experimental interface development. A. Mean plot heights ($cm$) by month. Red, yellow, green, blue, and purple indicate, respectively, $L = 1, 2, 4, 8, 16$ $m$. "Noise" added to abscissa for visibility. B. Each plot's interface width by month; note the logarithmic axes. Dashed line indicates scaling of the first 4 months (development). Estimated growth exponent $\beta = 0.31$. 1 $m$ plots marked as X, signifying earlier saturation; see text.

treated data from June through August as the interface-development period, and treated data from September (month 4) as stationary. This is an approximation, since correlation lengths for larger values of $L$ continued to grow during October.

## 4.1 Spatial correlation

Spatial correlations between row heights $h_y(t)$ both increased in strength and extended to greater distances along the interface as clover advanced. Since development of correlation length should not depend on $L$, we pooled observations from all plots. We estimated correlation $G_t(l)$ between row heights $h_y(t)$, as a function of distance, for each of the five months. Figure 4A shows the resulting correlogram; spatial correlation increased every month across most distances less than 200 $cm$.

The height-difference correlation $C_t(l)$ corroborated the pervious result; see Figure 4B. Each month $C_t(l)$ scaled as a power law for an increasing distance along the interface. Using the result for month 4, our model selection procedure strongly supported a power-law relationship with multiplicative error (Table 3). Power-law behavior of the height-difference correlation allows an estimate of the roughness exponent, since $C_t \sim l^{\alpha}$, for $l < \xi(t)$.

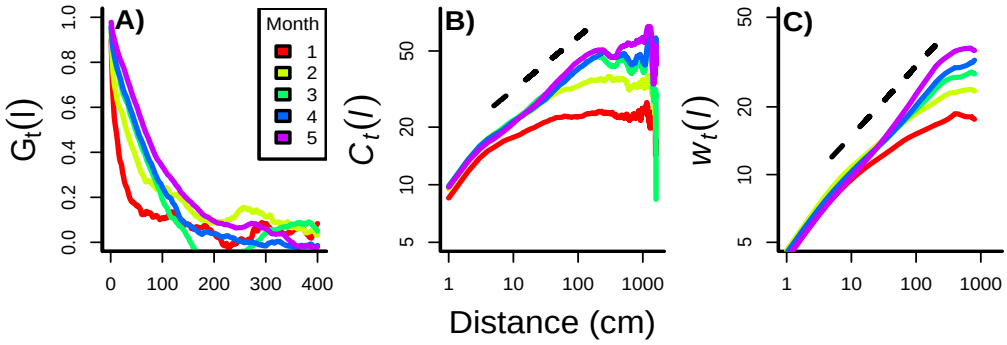


Figure 4: Interface development, field experiment. A. Spatial correlogram: correlation of row heights, $G_t(l)$. The strength and lag distance at which correlations $G_t(l)$ remained significant increased through time, indicating increasing correlation length $\xi(t)$ along the interface. Key indicates month 1 through 5; plots combined. B. Height-difference correlation function, $C_t(l)$, for months 1 through 5, plots combined. Distance over which power-law scaling holds increases with time; that is, distance along the front over which the log-log plot remains linear increases as correlation distance increases. Dashed line indicates month-4 scaling: $\alpha = 0.277$. C. Local interface width $w_t(l)$ across months. The dashed line indicates the scaling relationship for month 4, where the estimated roughness exponent was $\alpha = 0.311$.

Regression analysis of the $C_t(l)$ results yielded $\alpha = 0.277 \pm 0.002$; see Figure 4B.

## 4.2 Front roughening

As the interface roughens, its width should increase with time according to $\langle w^2(L,t)\rangle^{1/2} \sim t^{\beta}$. Figure 3B shows each plot's interface width against time. We tested the predicted scaling after excluding data for $L = 1\ m$, since roughening in those (smallest) plots equilibrated earlier than observed for larger $L$. Model selection found support for the power-law model with multiplicative error (Table 3). Using this model, we estimated the growth exponent $\beta$ as $0.34 \pm 0.12$ (mean $\pm$ 95% confidence interval; $R^2 = 0.355$). Inclusion of plots where $L = 1\ m$ had little effect; the resulting estimate is $\beta = 0.313$; see Figure 3B.

Figure 4C shows how scaling of the local interface widths $w_t(l)$ extended further as the interface roughened. Each month $w_t(l)$ scaled as the same power law for a greater distance along the interface.

| Clover Growth Analysis | Linear | Exp 1 | Exp 2 | Pow 1 | Pow 2 |
|---|---|---|---|---|---|
| $w^2(t)$ | 411.21 | 407.82 | 4.65 | 0 | 408.72 |
| $C(l)$ | 2014.94 | 1716.08 | 754.1 | 0 | 1398.53 |
| $w^2(l)$ | 3629.0 | 3061.25 | 1528.87 | 0 | 2528.99 |
| $w^2(L)$ | 118.44 | 117.02 | 2.56 | 0 | 117.18 |
| $\langle \Delta_{max} \rangle_L$ | 158.15 | 155.15 | 6.48 | 0 | 155.76 |

Table 3: $\Delta AIC$ scores. Models compared are as follows. Linear: $y = x + \epsilon$; Exp 1: $y = log(x) + \epsilon$; Exp 2: $log(y) = x + \epsilon$; Pow 1: $log(y) = log(a) + b\ log(x) + \epsilon$; Pow 2: $y = ax^b + \epsilon$. $\epsilon$ is a random error term with zero expectation and finite variance. Results support power-law models of Table 2.

We estimated interface velocity as the difference in monthly mean clover height. Combining all plots, clover advanced fastest during the first month of growth. September velocities (after roughening saturated) were independent of interface length $L$. After September, longer fronts continued to advance, but some shorter fronts receded as the growing season ended. During the period of interface roughening, overall mean clover height advance at 20 $cm/mo$. This exceeds mean stolen-elongation rates cited by Cain et al. [1995], but is within the observed range of clover "dispersal distances" discussed by Schwinning and Parsons [1996a]. Interface velocity appeared more sensitive to seasonal effects than did the roughened structure of the interface.

### 4.3 Stationary roughness and the front-runner: power laws

Assuming that roughening equilibrated in month 4, we tested the predicted scaling form against alternatives in two ways; each used the final month's data. The first test uses the local roughening analysis, and the second asks how mean interface width increases with $L$.

After saturation, the local width $w(l)$, where $(l \leq L)$, should scale as $w(l) \sim l^{\alpha}$. We combined month-4 data from different plots to characterize local roughening; see Figure 4C. Our AIC-criterion strongly supported the power-law formulation with multiplicative

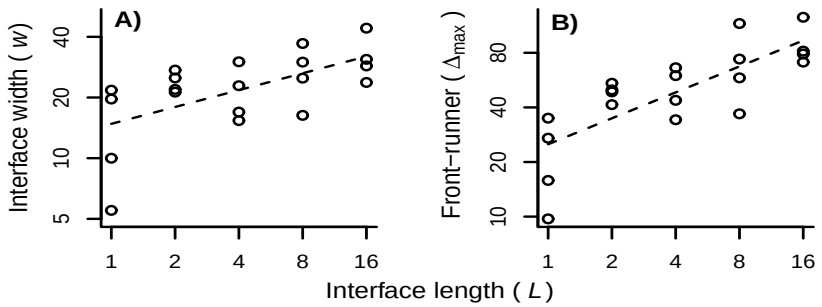


Figure 5: Saturated roughening. A. Interface widths ($cm$)for different front lengths $L$, data from September (month 4). Dashed line indicates power-law scaling. B. Front-runner's lead ($\Delta_{max}$), in $cm$, for different interface lengths $L$; data from month 4. Dashed line indicates power-law scaling.

error (Table 3). The associated estimate of the roughness exponent was $\alpha = 0.311 \pm 0.002$.

The mean roughening analysis treated each plot's width $w(L)$ separately. Using September estimates (see Figure 5A), the model selection procedure again provided substantial support for a power-law relationship with multiplicative error (Table 3). The power-law model for mean interface width as a function of interface length gave an estimate $\alpha$ as $0.278 \pm 0.18$.

Once roughening has equilibrated, the average lead of the front-runner, beyond the mean interface height, should scale with length as $\langle \Delta_{max} \rangle_L \sim L^{\alpha}$. Our model selection procedure once again found support for power-law scaling with multiplicative error (Table 3). Using the preferred model, the front-runner scaling estimated the roughening exponent as $\alpha = 0.475 \pm 0.19$; $R^2 = 0.6$; see Fig. 5B.

| Scaling | Estimate ± 95% CI | Months |
|---|---|---|
| $C_t(l) \sim l^{\alpha}$ | $\alpha = 0.277 \pm 0.002$ | 1 - 5 |
| $w(l) \sim l^{\alpha}$ | $\alpha = 0.311 \pm 0.002$ | 4 |
| $w(L) \sim L^{\alpha}$ | $\alpha = 0.278 \pm 0.18$ | 4 |
| $\langle \Delta_{max} \rangle \sim L^{\alpha}$ | $\alpha = 0.475 \pm 0.19$ | 4 |
| $w(t) \sim t^{\beta}$ | $\beta = 0.34 \pm 0.12$ | 1 - 5 |

Table 4: Estimates of scaling exponents. The first column indicates the predicted scaling law; the second shows th numerical result. Months 1 - 5 consider development; month 4 assumes equilibrated roughening. $\alpha$ is the roughness exponent, and $\beta$ is growth exponent.

Table 4 lists values of the scaling exponents inferred from the clover-interface data. The length-based estimates of the roughness exponent $\alpha$ are consistent; scaling of the front-runner suggests greater roughness; see see Appendix B. But every statistical analysis involving either the growth or the roughness exponent supported a power-law formulation over alternative linear and exponential models, as follows from kinetic-roughening theory.

## 5 Interface profiles and local interactions

Interface geometry affects contact frequency between spatially clustered competitors, and exclusion *versus* coexistence can depend on interactions at the interface [Chesson and Neuhauser 2002, Allstadt et al. 2007]. A rougher interface (larger $\alpha$) might therefore accelerate local population dynamics, driving invasive advance. The more obvious interface attribute is the width; $w \sim L^{\alpha}$. As long as greater roughening does not increase local density of empty sites, a larger interface width increases interdigitation of invader and resident, so that the density of asymmetric competitive interactions will increase.

To emphasize the role of width $w_t$, we examine experimental interface profiles, plots of the fraction of $L$ rows occupied by clover as a function of distance from the current mean height. Figure 6 shows interface profiles from one experimental plot (16 $m$, same as Fig. 1) for five months. Every month clover and ryegrass occurred with nearly equal frequency at the mean height. The first month's (June) profile drops sharply; the competitors mix very little as the interface begins to develop. Closer to saturation, the profiles show that interface width increases, and the species mix at the neighborhood scale.

We approximated observed interface profiles with the complementary error function. If

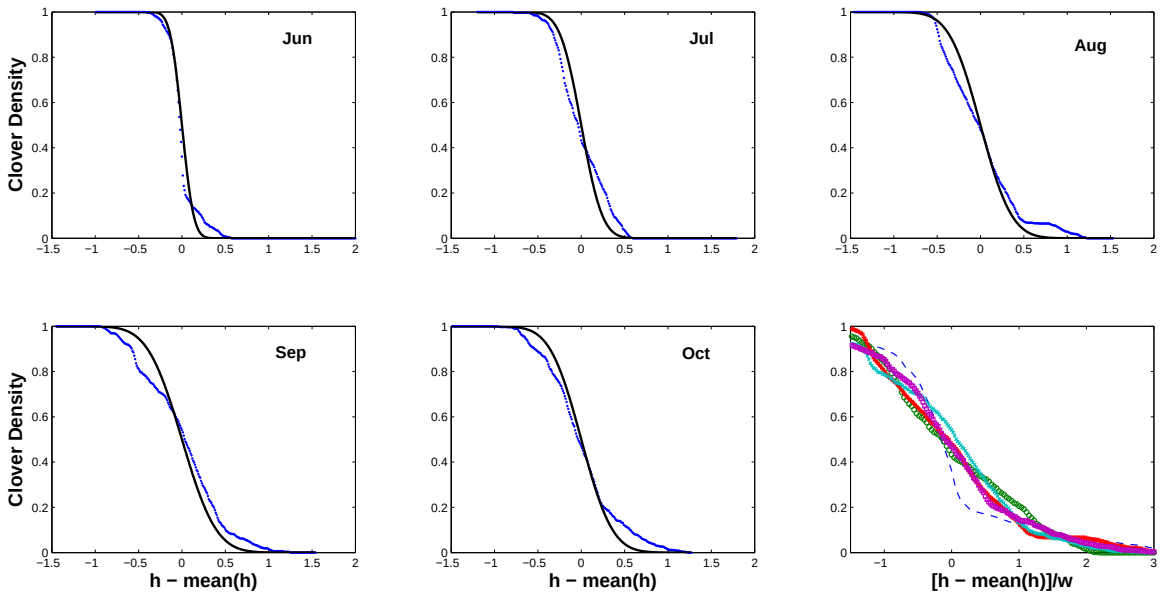


Figure 6: Density profiles of interface width, June through October (as indicated). $L = 16\ m$. Each month's empirical profile indicated by (•). Associated complementary error function for each month, parameterized by observed width, approximates data. Interface widths for consecutive month are, respectively, $w = 0.15, 0.27, 0.4, 0.44, 0.4$. Lower right. Data collapse. Dividing height (relative to front's mean position) by width indicates that last four months' clover-density profiles share structural organization. First month (broken line) insufficiently roughened to "fit." Symbols are empty circle (Jul), square (Aug), × (Sep) and closed circle (Oct).

330 $\rho_t(h)$ represents clover density at height $h$ and time $t$. Then:

$$\rho_t(h) = \frac{1}{2}\ erfc\left([h - \overline{h}(t)])/w_t\right) \tag{5}$$

where $w_t$ is interface width estimated at time $t$. The complementary error function is:

$$erfc\ (x) = \frac{2}{\sqrt{\pi}} \int_x^\infty exp\left[-z^2\right] dz$$

332 Equation 5 reasonably approximates observed profiles, since mean invader density has a roughly Gaussian decline across the interface; see Foltin et al [1994].

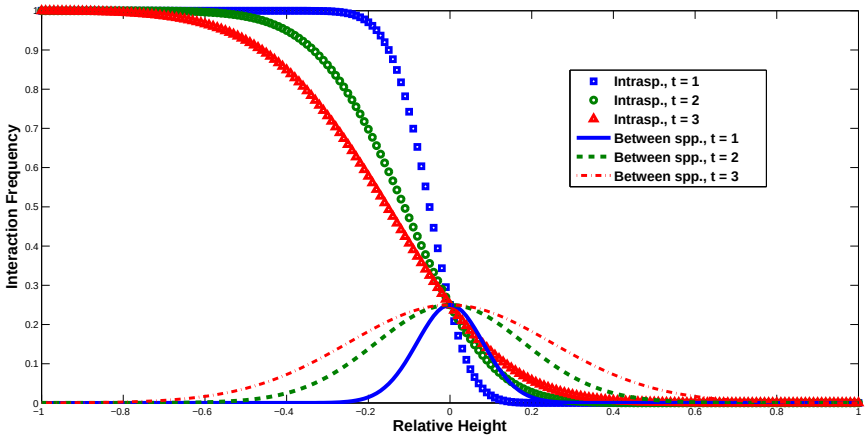


Figure 7: Invader interaction frequencies. $w(t = 1) = 0.15$ (blue), $w(t = 2) = 0.27$ (green), and $w(t = 3) = 0.4$ (red). As time advances, interface width increases. As width increases, (1) decline in intraspecific competition behind mean height exceeds increase in intraspecific competition in front of mean height, and (2) interspecific competition increases symmetrically about mean height.

The final subplot in Fig. 6 (lower right) indicates "data collapse" of the last four months' density profiles. Re-scaling height as $[h - \overline{h}(t)])/w_t$ reveals that the profiles share a common structural dependence on interface width, close to/at saturation. That is, the re-scaled plot shows a basic relationship for which the July through October profiles are examples. The first profile, a relatively un-roughened interface, has a different dependence.

Interface profiles neglect open sites and average across spatially correlated invader density, but indicate how biotic interactions are organized within the interface. If intraspecific interactions occur at height $h$ in proportion to $[\rho_t(h)]^2$, their frequency will decline faster than invader frequency within the interface width. Interspecific interactions, if proportional to $\rho_t(h)[1 - \rho_t(h)]$, will increase initially, peak at $\overline{h}(t)$, and then decline. Given this approximation, greater roughening increases interspecific mixing at the interface in a quantifiable manner; see Figure 7. Extending this basic picture, we can ask how interface width affects, and is affected by, ecological detail. For example, when within and between-species effects act across differently sized neighborhoods [Murrell and Law 2003],

348 or when dispersal-limited parasites prefer one of two competing hosts [Borer et al. 2007], interface geometry might modulate local population dynamics.

## 350 6 Discussion

Clonal organisms dominate many communities [Gough et al. 2002, Kui et al. 2013], so that 352 dispersal limitation must often generate clustered growth patterns. Consequently, invasive growth and competitive interactions may commonly occur within the width of an ecological 354 interface, where interaction neighborhoods overlap. Our general depiction of spatial competition, common to numerous detailed models, invites application kinetic-roughening 356 theory as a way to understanding pattern and process in the spatial structure of dispersal-limited organisms.

358 In our field experiment, clover advanced, displacing ryegrass. Simultaneously, clover's spatial correlation length along the interface increased. After a self-affine interface has 360 saturated, the fractal exponent $D$ is given by $D = 2 - \alpha$. Taking our length-based estimates of $\alpha$, we have $D \approx 5/3$; cover growth we observed "fills space" more than 362 predicted by a model where invader and resident grow froward and laterally at the same rate [O'Malley et al. 2006]. That is, lattice models for clonal growth usually assume that 364 an individual (ramet) will propagate forward, backward and laterally; any unoccupied, nearest-neighboring site can be colonized at the same stochastic rate. But Cain et al. 366 [1995] carefully mapped the architecture of clonal growth in a white clover population. Node-to-node branching angles of apical meristems centered on 0° (straight ahead), but 368 some large angles were observed. Lateral meristems branched off with a bimodal angular distribution, concentrated at $\pm 60 - 70°$. Clover, then, exhibits forward and lateral growth,

but with a bias toward forward propagation. The resulting morphology could have induced the difference between the scaling of the front-runner's lead and the scaling of interface roughening.

We studied an interface at the level of clustered individuals competing for space; a lattice site in our field experiment had area $1cm^2$. Cannas et al. [2004] invoked kinetic roughening in analyzing an individual-based simulation of an invasive tree advancing into a forest; they assumed each site had area $25m^2$. The methods of kinetic roughening should apply beyond individual-based scales. For example, expansion or contraction of a species' geographic range might be characterized as interface movement between habitats, driven by gain and loss of local demes. The obvious complication across greater distances is ecological heterogeneity [Gastner et al. 2009]. Spatial heterogeneity in demographic rates, varying at a scale much greater than local dispersal distance, implies that the roughness exponent $\alpha$ will vary along the length of an extended interface. In this case the front has a multi-affine, or turbulent, structure, and local estimates of roughness will not predict larger-scale behavior [Barabási and Stanley 1995]. More generally, spatial heterogeneity, whether fixed or temporally variable, can affect the likelihood an invasion begins [O'Malley et al. 2010] and front velocity when invasion succeeds [Shigesada et al. 1986].

**ACKNOWLEDGEMENTS**. We thank K. Bolton, K. Shukla, and the staff at the Guelph Turfgrass Institute and Research Station for help with the experiment. We appreciate comments by G. Robinson, L. O'Malley, A.J. Parsons and A.C. Gorski. This material is based upon research supported by the National Science Foundation under Grant No. DEB 0918392 (TC), DEB 0918413 (GK), and DMR 1246958 (GK); field research was supported by grants from the Ontario Ministry of Agriculture (JAN) and the Canadian Natural Sciences and Engineering Research Council (JAN).

# References


[Allstadt et al. 2007] Allstadt A, Caraco T, Korniss G (2007) Ecological invasion: spatial clustering and the critical radius. *Evol Ecol Res* 9:375–394.

[Allstadt et al. 2009] Allstadt A, Caraco T, Korniss G (2009) Preemptive spatial competition under a reproduction-mortality constraint. *J Theor Biol* 258:537–549.

[Allstadt et al. 2012] Allstadt, A, Caraco T, Molnár F, Jr, Korniss G (2012) Interference competition and invasion: spatial structure, novel weapons, and resistance zones. *J Theor Biol* 306:46–60.

[Antonovics et al. 2006] Antonovics J, McKane AJ, Newman TJ (2006) Spatiotemporal dynamics in marginal populations. *Am Nat* 167:16–27.

[Barabási and Stanley 1995] Barabási A-L, Stanley HE (1995) *Fractal Concepts in Surface Growth*. Cambridge University Press, Cambridge (UK). 386 p.

[Borer et al. 2007] Borer ET, Hosseini PR, Seabloom EW, Dobson AP (2007) Pathogen-induced reversal of native dominance in a grassland commmunity. *Proc Natl Acad Sci USA* 104:5473–5478.

[Burnham and Anderson 2002] Burnham KP, Anderson, DR (2002) *Model selection and multimodel inference: a practical information-theoretic approach* Springer Verlag, Heidelberg.

[Cain et al. 1995] Cain ML, Pacala SW, Silander JA, Jr, Fortin M-J (1995) Neighborhood models of clonal growth in the white clover *Trifolium repens*. *Am Nat* 145:888–917.

[Cannas et al. 2004] Cannas SA, Marco DE, Páez SA, Montemurro MA (2004) Plant spread dynamics and spatial patterns in forest ecology. *Interdisciplinary Applications of Ideas from Nonextensive Entropy*, eds Gell-Mann M, Tsallis C (Santa Fe Institute). 16 pp.

[Cantor et al. 2011] Cantor A, Hale A, Aaron J, Traw MB, Kalisz S (2011) Low allelochemical concentrations detected in garlic mustard-invaded forest soils inhibit fungal growth and AMF spore germination.*Biol Invas* 13:3015–3025.

[Chesson 2000] Chesson P (2000) Mechanisms of maintenance of species diversity. *Ann Rev Ecol Syst* 31:343–366.

[Chesson and Neuhauser 2002] Chesson P, Neuhauser C (2002) Intraspecific aggregation and species coexistence. *Trends Ecol Evol* 17:210–211.

[Clark et al. 2001] Clark JS, Lewis M, Horvath L (2001) Invasion by extremes: population spread with variation in dispersal and reproduction. *Am Nat* 157:537–554.

[Clark et al. 2003] Clark JS, Lewis M, McLachlan JS, HilleRisLambers J (2003) Estimating population spread: what can we forecast and how well? *Ecology* 84:1979–1988.

[Condit et al. 2000] Condit R, Ashton PS, Baker P, Bunyavejchewin S, Gunatilleke S, et al (2000) Spatial patterns in the distribution of tropical tree species. *Science* 288:1414–1418.

[Dale 1999] Dale MRT (1999) *Spatial Pattern Analysis in Plant Ecology*. Cambridge University Press, Cambridge, UK Theoretical Population Biology 46:363–394.

[Eppinga et al. 2013] Eppinga MB, Pucko CA, Baudena M, Beckage B, Molofsky J (2013) A new method to infer vegetation boundary movement from 'snapshot' data. *Ecography* 36:622–625.

[Escudero et al. 2004] Escudero C, Buceta J, de la Rubia FJ, Lindenberg K (2004) Extinction in population dynamics. *Phys Rev E* 69:021908, 9 pp.

[Family and Vicsek 1985] Family F, Vicsek T (1985) Scaling of the active zone in the Eden process on percolation networks and the ballistic deposition model. *J Physics A* 18:L75-L81.

[Fisher and Tippett 1928] Fisher RA, Tippett LHC (1928) The frequency distribution of the largest or smallest member of a sample. *Proc Cambridge Phil Soc* 24:180–191.

[Foltin et al. 1994] Foltin G, Oerding K, Rácz Z, Workman RL, Zia RKP (1994) Width distribution for random-walk interfaces. *Phys Rev E* 50:R639–R642.

[Fraser 1989] Fraser J (1989) Characteristics of naturalized populations of white clover (*Trifolium repens*) in Atlantic Canada. *Can J Botany* 67:2297–2301.

[Fustec et al. 2005] Fustec J, Guilleux J, Le Corff J, Maitre JP (2005) Comparison of early development of three grasses: *Lolium perenne*, *Agrostis stolonifera* and *Poa pratensis*. *Ann Botany* 96:269–278.

[Galambos et al. 1994] Galambos J, Lechner J, Simin E, eds (1994) *Extreme Value Theory and Applications* (Kluwer, Dordrecht).

[Galeano et al. 2003] Galeano J, Buceta J, Juarez K, Pumarino B, de la Torre J, Iriondo JM (2003) Dynamical scaling analysis of plant callus growth. *Europhys Lett* 63:83–89.

[Gandhi et al. 1999] Gandhi A, Levin S, Orszag S (1999) Nucleation and relaxation from meta-stability in spatial ecological models. *J Theor Biol* 200:1221–146.

[Gastner et al. 2009] Gastner MT, Oborny B, Zimmermann DK, Pruessner G (2009) Transition from connected to fragmented vegetation across an environmental gradient: scaling laws in ecotone geometry. *Am Nat* 174:E23–E39.

[Goldberg and Barton 1992] Goldberg DE, Barton AM (1992) Patterns and consequences of interpsecific competition in natural communities: a review of field experiments with plants. *Am Nat* 139:771–801.

[Gough et al. 2002] Gough L, Goldberg DE, Hershock c, Pauliukonis N, Petru M (2002) Investigating the community consequences of competition among clonal plants. *Evol Ecol* 15:547–563.

[Hajek et al. 1996] Hajek AE, Elkinton JS, Witcosky JJ (1996) Introduction and spread of the fungal pathogen *Entomophaga maimaiga* (Zygomycetes:Entomophthorales) along the leading edge of Gypsy Moth (Lepidoptera:Lymantriidae) spread. *Envir Entomol* 25:1225–1247.

[Harada and Iwasa 1994] Harada Y, Iwasa Y (1994) Lattice population dynamics for plants with dispersing seeds and vegetative propagation. *Res Pop Ecol* 36:237–249.

[Herben et al. 2000] Herben T, During HJ, Law R (2000) Spatio-temporal patterns in grassland communities. *The Geometry of Ecological Interactions*, eds Dieckmann U, Law R, Metz JAJ (Cambridge University Press, Cambridge). pp. 48–64.

[Karabacak et al. 2001] Karabacak T, Zhao Y-P,Wang G-C, Lu T-M (2001) Growth-front roughening in amorphous silicon films by sputtering. *Phys Rev B* 64:085323, 10 pp.

[Kardar et al. 1986] Kardar M, Parisi G, Zhang Y-C (1986) Dynamic scaling of growing interfaces. *Phys Rev Lett* 56:889–892.

[Korniss and Caraco 2005] Korniss G, Caraco T (2005) Spatial dynamics of invasion: the geometry of introduced species. *J Theor Biol* 233:137–150.

[Korniss et al. 2000] Korniss G, Toroczkai Z, Novotny MA, Rikvold PA (2000) From massively parallel algorithms and fluctuating time horizons to nonequilibrium surface growth. *Phys Rev Lett* 84:1351–1354.

[Korniss et al. 2003] Korniss G, Novotny MA, Guclu H, Toroczkai Z, Rikvold PA (2003) Suppressing roughness of virtual times in parallel discrete-event simulations. *Science* 299:677–679.

[Krug and Meakin 1990] Krug J, Meakin P (1990) Universal finite-size effects in the rate of growth processes.*J Physics A* 23:L987, 9 pp.

[Kui et al. 2013] Kui L, Li F, Moore F, West J (2013) Can the riparian invader, *Arundo donax*, benefit from clonal integration? *Weed Res* 53:370–377.

[Levine et al. 2004] Levine JM, Adler PB, Yelenik SG (2004) A meta-analysis of biotic resistance to exotic plant invasions. *Ecol Lett* 7:975–989.

[Liu et al. 2006] Liu J, Dong M, Miao SL, Li ZY, Song MH, Wang RQ (2006) Invasive alien plants in China: role of clonality and geographical origin. *Biol Inv* 8:1461–1470.

[Majumdar and Comtet 2004] Majumdar SN, Comtet A (2004) Exact maximal height distribution of fluctuation interfaces. *Phys Rev Lett* 92:225501, 4 pp.

[Majumdar and Comtet 2005] Majumdar SN, Comtet A (2005) Airy distribution function: from the area under a Brownian excursion to the maximal height of fluctuating interfaces. *J Stat Phys* 119:776–826.

[Moro 2001] Moro E (2001) Internal fluctuations effects on Fisher waves. *Phys Rev Lett* 87:238303, 4 pp.

[Murrell and Law 2003] Murrell DJ, Law R (2003) Heteromyopia and the spatial coexistence of similar competitors. *Ecol Lett* 6:48–59.

[O'Malley et al. 2006] O'Malley L, Kozma B,Korniss G, Rácz Z, Caraco T (2006) Fisher waves and front propagation in a two-species invasion model with preemptive competition. *Phys Rev E* 74:041116, 7 pp.

[O'Malley et al. 2009a] O'Malley L, Korniss G, Caraco T (2009) Ecological invasion, roughened fronts, and a competitor's extreme advance: integrating stochastic spatial-growth models. *Bull Math Biol* 71:1160–1188.

[O'Malley et al. 2009b] O'Malley L, Kozma B, Korniss G, Rácz Z, Caraco T (2009) Fisher waves and the velocity of front propagation in a two-species invasion model with pre-

emptive competition. *Computer Simulation Studies in Condensed Matter Physics XIX*, eds Landau DP, Lewis SP, Schüttler H-B (Springer, Heidelberg). pp. 73-78.

[O'Malley et al. 2010] O'Malley L, Korniss G, Mungara SSP, Caraco T (2010) Spatial competition and the dynamics of rarity in a temporally varying environment. *Evol Ecol Res* 12:279–305.

[Pachepsky and Levine 2011] Pachepsky E, Levine JM (2011) Density dependence slows invader spread in fragmented landscapes. *Am Nat* 177:18–28.

[Pechenik and Levine 1999] Pechenik L, Levine H (1999) Interfacial velocity corrections due to multiplicative noise. *Phys Rev E* 59:3893–3900.

[Plischke et al. 1987] Plischke M, Rácz Z, Liu D (1987) Time-reversal invariance and universality of two-dimensional models. *Phys Rev B*:3485–3495.

[Ranft et al. 2014] Ranft J, Allee M, Prost J, Jülicher J, Joanny J-F (2014) Mechanically driven interface propagation in biological tissues. *New J Physics* 16:035002, 10 pp.

[Sakai et al. 2001] Sakai AK, Allendorf FW, Holt JS, Lodge DM, Molofsky J, With KA, Baughman S, Cabin RJ, Cohen JE, Ellstrand NC, McCauley DE, O'Neil P, Parker IM, Thompson JN, Weller SG (2001) The population biology of invasive species. *Ann Rev Ecol Syst* 32:305–332.

[Schehr and Majumdar 2006] Schehr G, Majumdar SN (2006) Universal asymptotic statistics of a maximal relative height in one-dimensional solid-on-solid models. *Phys Rev E* 73:056103, 10 pp.

[Schwinning and Parsons 1996a] Schwinning S, Parsons AJ (1996) A spatially explicit population model of stoloniferous N-fixing legumes in mixed pasture with grass. *J Ecol* 84:815–826.

534 [Schwinning and Parsons 1996b] Schwinning S, Parsons AJ (1996) Analysis of coxistence mechanisms for grasses and legumes in grazing systems. *J Ecol* 84:799–813.

536 [Shigesada et al. 1986] Shigesada N, Kawasaki K, Teramoto E (1986) Travelling periodic waves in heterogeneous evironments. *Theor Pop Biol* 30:143–160.

538 [Silvertown 1981] Silvertown JW (1981) Micro-spatial heterogeneity and seedling demography in species-rich grassland. *New Phytologist* 88:117–128.

540 [Snyder and Chesson 2003] Snyder RE, Chesson P (2003) Local dispersal can facilitate coexistence in the presence of permanent spatial heterogeneity. *Ecol Lett* 6:301–309.

542 [Solow et al. 2003] Solow AR, Costello CJ, Ward M (2003) Testing the power law model for discrete size data. *Am Nat* 162:6785–689.

544 [Thomson and Ellner 2003] Thomson NA, Ellner SP (2003) Pair-edge approximation for heterogeneous lattice population models. *Theor Pop Biol* 64:270–280.

546 [Turkington et al. 1979] Turkington R, Cahn MA, Vardy A, Harper JL (1979) The growth, distribution and neighbour relationships of *Trifolium repens* in a permanent pasture: 548 III. The establishment and growth of *Trifolium repens* in natural and perturbed sites. *J Ecol* 67:231–243.

550 [van den Bosch et al. 1992] van den Bosch F, Hengeveld R, Metz JAJ (1992) Analysing the velocity of animal range expansion. *J Biogeo* 19:135-150.

552 [Xiao et al. 2011] Xiao X, White EP, Hooten MB, Durham SL (2011) On the use of log-transformation vs. nonlinear regression for analyzing biological power laws. *Ecology* 554 92:1887–1894.

[Yurkonis and Meiners 2004] Yurkonis KA, Meiners SJ (2004) Invasion impacts local species 556 turnover in a successional ecosystem. *Ecol Lett* 7:764–769.